Journal of
Materials Chemistry C

Accepted Manuscript

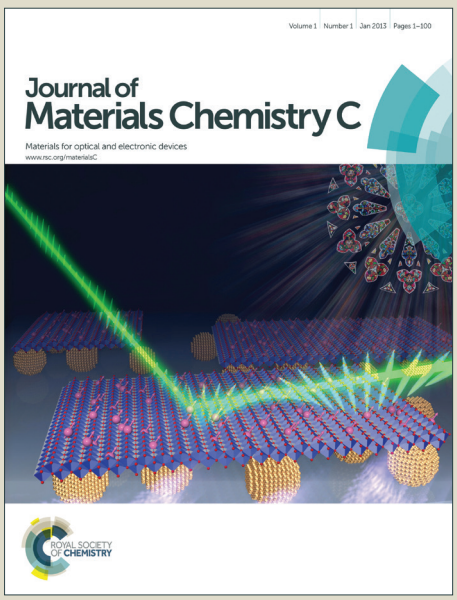




ROYAL SOCIETY OF CHEMISTRY

www.rsc.org/materialsC

Journal Name RSCPublishing

ARTICLE

# Light-driven Fluorescence Enhancement and Self-assembled Structural Evolution of an Azobenzene Derivative

Cite this: DOI: 10.1039/x0xx00000x

Received 00th January 2012,
Accepted 00th January 2012

DOI: 10.1039/x0xx00000x

www.rsc.org/

Xia Ran[a], Haitao Wang[b], Lili Shi[a], Jie Lou[a], Bo Liu[a], Min Li[b], and Lijun Guo*[a]

Achieving fluorescent azobenzene derivative and investigating the relationship between the self-assembled structure and photophysical property is a challenging topic and of significance in material science. Here, we report the light-driven fluorescence enhancement and self-assembled structural characteristics of an azobenzene derivative N-(3,4,5-octanoxyphenyl)-N'-4-[(4-hydroxyphenyl)azophenyl] 1,3,4-oxadiazole (AOB-t8). A highly fluorescent self-assembled aggregate of *cis*-AOB-t8 in organic solution under UV light illumination has been observed, the quantum yield can reach $33.7\times10^{-2}$, up to 306 times enhancement compared with that of *trans*-AOB-t8 which is negligibly fluorescent in nonirradiated initial solution. It has been proposed that the fluorescence enhancement originates from the *trans*-to-*cis* monomeric isomerization and the aggregate of *cis*-AOB-t8. Based on the theoretical calculations, we have discussed the mechanism for light-driven fluorescence enhancement of monomeric *cis*-AOB-t8, which is applied commendably to interpret the observed spectroscopic result. On the other hand, the formation of J-aggregate of *cis*-AOB-t8 is the origination of further emission enhancement. Meanwhile, this photocontrolled fluorescence enhancement in concentrated solution ($1\times10^{-3}$ M) could be attributed to the significant structural changes of aggregates, from fiber-like aggregates to layer structure aggregates. According to the spectroscopy study, it is suggested that the *trans*-AOB-t8 is inclined to form H-aggregate and the *cis*-AOB-t8 to form J-aggregate, which could probably lead to the structural variety related to different molecular conformation of AOB-t8.

## Introduction

Azobenzene and its derivatives are well known for their photochromic properties, as they can undergo photoinduced *trans-cis* isomerization. These compounds are widely used as photo-responsive materials,[1-4] such as optical data storage, liquid crystal display, optical switching, holographic surface relief grating, etc. However, in general, it is a known fact that azobenzene molecules do not fluoresce in solution with imperceptible quantum yield due to the *trans-cis* isomerization.[5-6] On the other hand, emitting azobenzenes have been expected to be powerful candidates as fluorescent materials applying to light-emitting devices, fluorescent probes, and molecular detectors, because of the variety of archived methods for synthesizing azobenzenes and tuning their properties. Recently, a few reports have been represented on fluorescence emission in different systems, such as acidification of azobenzene chromophores,[7,8] boron-substituted azobenzene,[9] the self-assembled bilayer aggregates[10,11] and the light induced self-assembly of *cis*- azobenzene moieties.[12,13] Yoshino and co-workers reported several 2-borylazobenzenes emitting an intense green, yellow, and orange fluorescence, in marked contrast to the negligible azobenzene fluorescence. The 4'-siloxy derivative showed the highest fluorescence quantum yield of 0.90 among those reported azobenzene derivatives to date.[9] De Schryver and co-workers reported the vesicles containing azobenzene units fluoresce with a maximum emission at 600 nm, which was attributed to the dense and ordered arrangement of the azobenzene chromophores in the bilayer structure.[11] Han and co-workers observed the photoinduced formation of blue fluorescent aggregates in 460-500 nm region for simple azobenzene derivatives with different alkyl chain lengths, whose isolated molecules in solution were nonfluorescent at ambient temperature.[12]

The mechanisms of emission for monodispersed solution are mostly accepted to be the origin of an inhibition of photoinduced electron transfer (PET),[14,15] the restriction effects on nonradiative relaxation process of the *trans*-to-*cis* isomerization of azobenzene groups.[11,16,17] Zacharias et al.[14] and Smitha and Asha[15] reported the fluorescent enhancement accompanied by isomerization from nonaggregated azobenzene solution bearing fluorophores, and proposed that the inhibiting photoinduced electron transfer is the origination of enhanced luminescence due to the nonplanar geometry in the *cis*- isomer of the azobenzene group. Yoshino et al. suggested that the suppression locks the photoisomerization process around the N=N double bond, which is responsible for the very efficient radiationless deactivation in the unsubstituted azobenzene, and

helps provide the boron-substituted azobenzene with the extremely high fluorescence quantum yield.[9] Meanwhile, Han et. al proposed that the photoinduced fluorescence enhancement is attributed to light driven self-assembly of *cis*- azobenzenes.[12] Up to now, a complete mechanism of fluorescent emission of azobenzene derivatives is still beyond our understanding. It is essential to further explore fluorescent azobenzene-containing derivatives with a deep investigation on the cause of fluorescence behaviour.

In this work, we focus on the photocontrolled photophysical property and self-assembly structural characteristics of the tapered molecule, N-(3,4,5-octanoxyphenyl)-N'-4-[(4-hydroxyphenyl)azophenyl] 1,3,4-oxadiazole (AOB-t8) (Scheme 1), which had been synthesized and reported in our previous work.[18] The highly fluorescent self-assembled plate aggregates of azobenzene molecules under UV light illumination was observed, even though *trans*- azobenzene itself is negligibly fluorescent in nonirradiated initial solution. We report here the significant structural characteristics of aggregates, from fiber-like aggregates to layer structure aggregates. Combining of spectroscopic techniques and theoretical calculations, we have discussed the possible mechanism for light-driven fluorescence and aggregation induced emission enhancement in this paper.

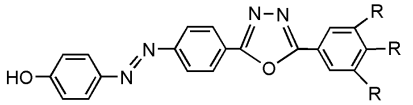


*trans*-AOB-t1: R=-$OCH_3$, *trans*-AOB-t8: R=-$OC_8H_{17}$

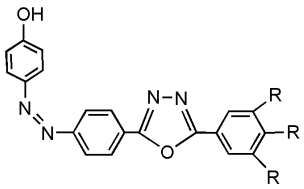


*cis*-AOB-t1: R=-$OCH_3$, *cis*-AOB-t8: R=-$OC_8H_{17}$

**Scheme 1** Molecular structure of AOB-t1 and AOB-t8.

## Results and discussion

### Photophysical properties

AOB-t8 demonstrates a good solubility in various organic solvents of moderate and strong polarity, and slight solubility in non-polar solvents. As shown in Fig. 1a and Table 1, AOB-t8 in dilute solution ($1\times10^{-5}$ M) shows an intense absorption around 354 nm in cyclohexane (CHEX), as well as a weak band around 450 nm. The high absorption intensity of shorter-wavelength band indicates a π-π* type absorption band of the *trans*-azobenzene moieties, which is consistent with the result obtained in the computational study (see below). The position of the absorbance maximum is slightly dependent on the polarity of solvents, from cyclohexane (CHEX) to tetrahydrofuran (THF) and dimethylformamide (DMF), with a total red-shift about 19 nm. The electronic and structural nature of the ground state and Franck-Condon (FC) excited state is responsible for these absorptions.

AOB-t8 exhibits a weaker emission feature like most *trans*-azobenzene derivatives. The fluorescence spectra of AOB-t8 in various solvents are shown in Fig. 1b and summarized in Table 1. In non-polar CHEX, AOB-t8 shows a stronger emission band around 362 nm with a vibrational fine structure (maximum at 348 and 376 nm, Fig. 1b).

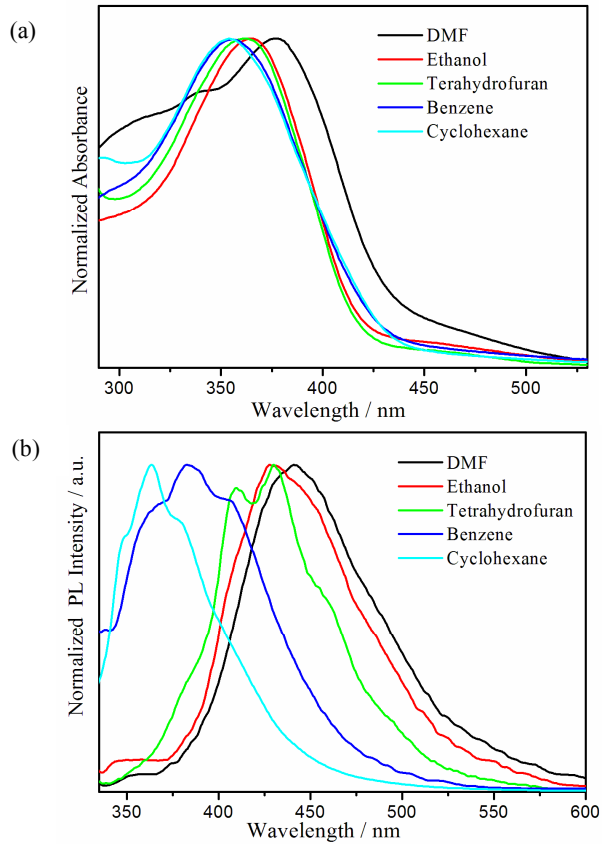


**Fig. 1** Normalized (a) UV-vis absorption and (b) fluorescence spectra of AOB-t8 ($1\times10^{-5}$ M) in different solvents.

**Table 1** Photophysical characteristics of *tans*-AOB-t8 ($1\times10^{-5}$ M) in different solvents at room temperature.

| Solvents | $\lambda_{abs}$ (nm) | $\lambda_{em}$ (nm) | Stokes shift ($cm^{-1}$) | $\Phi_F$ ($\times10^{-2}$) | τ (ns) |
|---|---|---|---|---|---|
| CHEX | 357 | 348,362,376 | 386.9 | 6.4 | 5.26 |
| Benzene | 358 | 361,385,403 | 1958.9 | 1.3 | 1.55 |
| THF | 363 | 428 | 4083.7 | 0.7 | 1.44 |
| ETO | 365 | 434 | 4018.4 | 0.2 | 2.15 |
| DMF | 376 | 443 | 4022.4 | 0.15 | 2.29 |

The fine structure is somewhat retained in solvents with moderate polarity (benzene and THF), and is totally lost in the highly polar solvents (ethanol (ETO) and DMF). This observation indicates the existence of strong solute-solvent interactions in the polar solvents, which broaden the vibronic transition and thus lead to the fine structure lost. Moreover, the emission spectra exhibit a large red-shift in their maxima from 362 nm (in CHEX) to 443 nm (in DMF) with increasing solvent polarity (Table 1 and Fig. 1b), while the fluorescence quantum yields decreased from $6.4\times10^{-2}$ (in CHEX) to $0.15\times10^{-2}$ (in

DMF) accompanying with the fluorescence lifetime from 5.26 ns to 2.29 ns (Fig. S1). The observations of the large red-shifted and decreased fluorescence emissions in the photoluminescence (PL) spectra in polar solvents implies the formation of intramolecular charge transitions and to some extent that the molecular dipole moment in the excited state is larger than the ground state.[19]

**Photoisomerization studies**

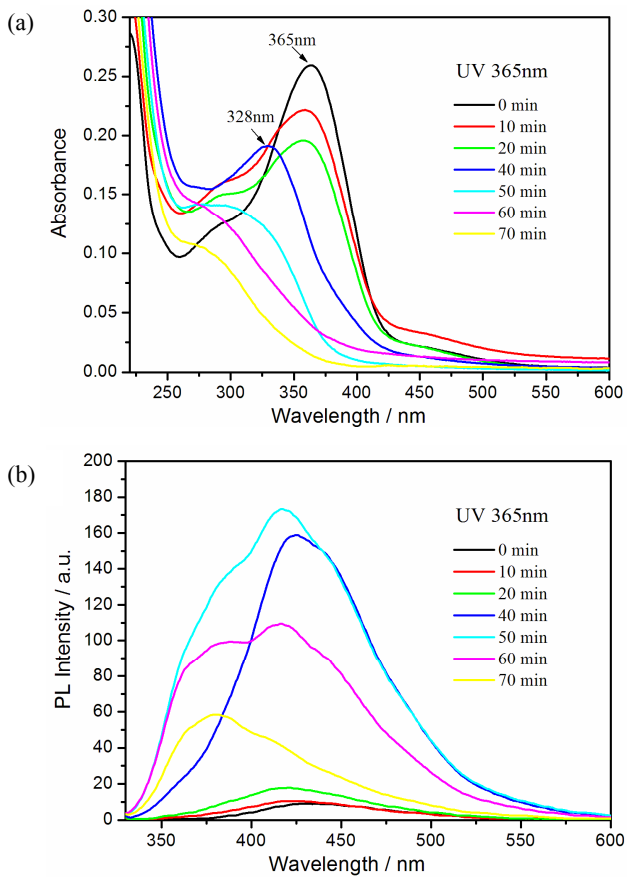


**Fig. 2** (a) UV-vis spectra and (b) fluorescence spectra of AOB-t8 in ETO ($1\times10^{-5}$ M) under irradiation at 365 nm for different time period at room temperature.

Photoisomerization is expected to induce the changes of photophysical properties of AOB-t8 both in monodispersed and aggregated states. In this work, the AOB-t8 was irradiated using the 365 nm band-pass filtered output from a 250 W high-pressure mercury lamp. UV-visible spectroscopy experiment of a $1\times10^{-5}$ M solution of AOB-t8 in ETO was carried out to monitor the photoirradiation process. The UV-vis spectra in Fig. 2a shows a typical evolution process that, the π-π* absorption of *trans*-azobenzene moiety at 365 nm decreases with the irradiation time, indicating that photoinduced *trans*-to-*cis* isomerization takes place. The conversion to *cis*- from *trans*-azobenzene reaches ca. 94% in the photostationary state after 70 min UV irradiation, which is estimated on the basis of the UV-vis absorption spectra.[20]

When a dilute ($1\times10^{-5}$ M) solution of AOB-t8 in ETO was excited at 320 nm, a very weak fluorescence with the maximum at 434 nm was observed, with a fluorescence quantum yield of $0.2\times10^{-2}$. However, an increasing fluorescence was activated after the solution was continuously exposed to UV light for 10 min, with the emission maximum blue-shifted to around 423 nm as shown in Fig. 2b, which can be attributed to the emission of monomeric *cis*-AOB-t8. With the increasing of UV light irradiation time from 10 to 50 min, a structural fluorescence spectrum clearly demonstrates an evolution feature of a significant band broadening and emission enhancing originated from the photoisomerization and the formation of *cis*-molecular aggregates. It can be seen that the broad emission band consists of three sub-bands after 50 min UV irradiation. One sub-band around 423 nm can be attributed to the emission of monomeric *cis*-AOB-t8. The other two blue-shifted sub-bands around 386 nm and 417 nm, respectively, were hypothesized to two kinds of *cis*-AOB-t8 aggregates with different size and structure. With UV light irradiation for 70 min, an apparent decreasing fluorescence can be observed in Fig.2b due the absorption section at this wavelength is getting smaller with time (see Fig.2a). In fact, the quantum yield is unceasingly improved to $5.8\times10^{-2}$, enhanced by 29 times than that of the nonirradiated initial solution. Meanwhile, the fluorescence spectrum after 70 min UV irradiation clearly demonstrates that the enhanced emission corresponding to the most blue-shifting band around 370 nm could mainly arise from the aggregate with bigger size.

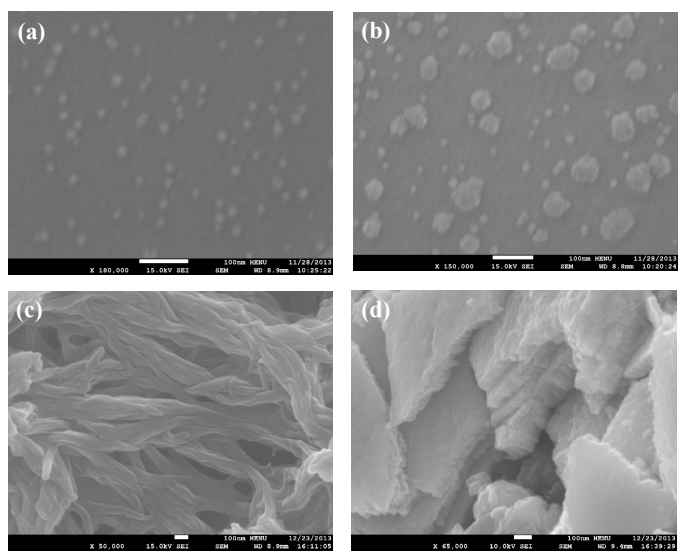


**Fig. 3** SEM images of AOB-t8 (a) in ETO ($1\times10^{-5}$ M) after exposure to UV light for 40 min, (b) 70 min, (c) in ETO ($1\times10^{-3}$ M) before exposure to UV light and (d) under irradiation at 365 for 290 min.

The results mentioned above demonstrate that the fluorescence enhancement probably correlates with the structure of molecular aggregation, which is so-called aggregation-induced emission enhancement (AIEE).[17] In order

to confirm that the observed spectral features are indeed due to aggregates during prolonged UV light irradiation, the topology structural investigation was carried out on scanning electron microscope (SEM). As shown in Fig. 3, the spherical aggregates of approximately 15-20 nm in diameter can be clearly resolved in the AOB-t8 samples after exposed to UV light for 40 min, and many more aggregates of approximately 15-90 nm in diameter are observed after 70 min. In contrast, such spherical aggregate is rarely formed in the samples exposed to UV light for less than 20 min. The SEM results are highly consistent with the dramatic changes in fluorescence intensity shown in Fig. 2b. The correlation between structural evolution and emission property of AOB-t8, strongly suggests that the striking fluorescence enhancement by UV light irradiation originates mainly from the formation of *cis*-AOB-t8 aggregates.

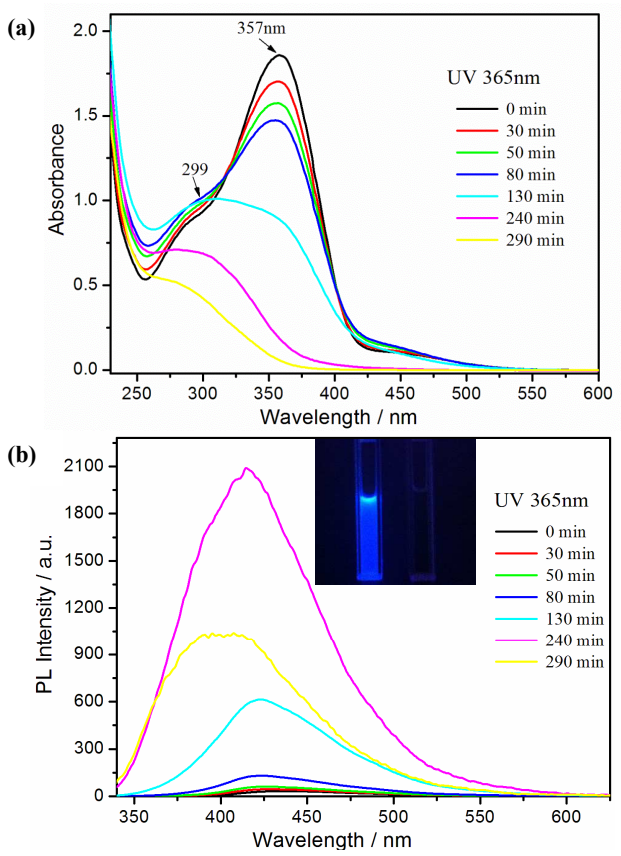


**Fig. 4** (a) UV-vis and (b) fluorescence spectra of AOB-t8 in ETO ($1\times10^{-3}$ M) under 365 nm irradiation for different time at room temperature.

To obtain deep insight into the self-assembled structure dependence of fluorescence enhancement, the photophysical properties of azobenzene solution with different concentrations ranging from $1\times10^{-5}$ to $1\times10^{-3}$ M were investigated. As shown in Table S1, without UV irradiation, the fluorescence quantum yield initially decreases with increasing concentration. The most concentrated solution ($1\times10^{-3}$ M) is almost nonfluorescent with the quantum yield of $1.1\times10^{-3}$ before UV light irradiation, due to the concentration quenching effect. In contrast to the case shown in Fig. 4b, the fluorescence spectrum exhibits a broad and blue-shifted band with the quantum yield of $33.7\times10^{-2}$ after UV light irradiation, up to 306 times emission enhancement. As we discussed in aforementioned photophysical properties of AOB-t8, it is demonstrated that the formation of an intramolecular charge transfer (ICT) state of *trans*-AOB-t8 in ETO is responsible for the emission quenching. The ICT is blocked to some extent in the case of *cis*-AOB-t8, resulting in the activation of emission enhancement. Within the aggregate state, the localized excited state of *cis*-AOB-t8 due to the restriction of intramolecular rotation and a different molecular arrangement might cause the intensified and blue-shifted emission. The photograph (inset of Fig. 4b) of the most concentrated solution ($1\times10^{-3}$ M) of AOB-t8 in ETO after UV light irradiation for 290 min displays a bright blue violet emission, presenting a marked contrast to the nonfluorescent one in the case without UV light irradiation.

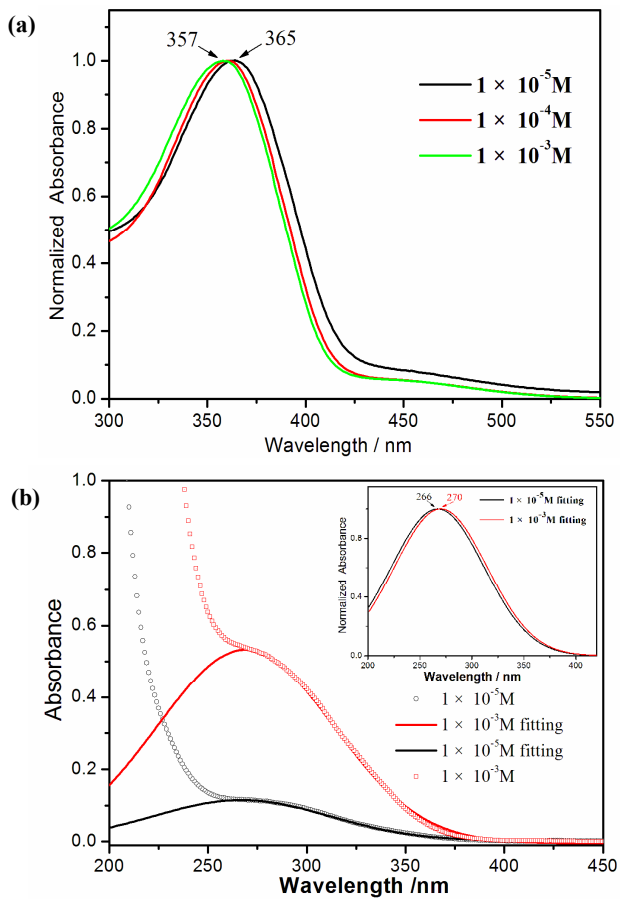


**Fig. 5** (a)Normalized UV-vis absorption spectra of AOB-t8 in ETO at different concentration, (b) original and fitting UV-vis absorption spectra of $1\times10^{-5}$ M (black) and $1\times10^{-3}$ M (red) in ethanol after 365 nm irradiation, respectively. Inset shows the normalized fitting curves.

This striking concentration dependence of emission appears to be closely associated with the size and structural changes of the aggregates induced by UV light irradiation. For comparison, the structural features of aggregates formed without and with UV irradiation are clearly shown in Fig.3. The SEM image in

Fig. 3c exhibits entangled and dense fibrous aggregates with an average diameter of 40-60 nm for $1\times10^{-3}$ M solutions before UV light irradiation. While as shown in Fig. 3d, a plate structure with the thickness of 70-80 nm can be observed for $1\times10^{-3}$ M solution after 365 nm UV irradiation for 290 min. This observation of morphology dependence on concentration of AOB-t8 in ETO demonstrates a photoinduced fiber-to-plate structure morphology evolution in coordination with solvent.

In order to explore the effect of solvent polarity on the self-assembled structure, we have investigated the light driven photophysical properties and aggregation pattern of AOB-t8 in dichloromethane. When a dilute ($1\times10^{-5}$ M) and concentrated ($1\times10^{-3}$ M) solution of AOB-t8 in dichloromethane were continuously exposed to UV light, an increasing fluorescence intensity was activated, which is similar to that of AOB-t8 in ethanol (Fig. S2 and Fig. S3). The quantum yield of AOB-t8 in dichloromethane ($1\times10^{-3}$ M) with UV light irradiation to balance state is unceasingly improved to $6.2\times10^{-2}$(enhancement factor is 134) which is less than that of AOB-t8 in ethanol (the quantum yield is $33.7\times10^{-2}$ and the enhancement factor is 306). Meanwhile, the response to UV light of AOB-t8 in dichloromethane is faster than that of AOB-t8 in ethanol. Similarly, the trans-to-cis isomerization of AOB-t8 in dichloromethane further causes the morphological change from fibers to nanoparticles as shown in Fig.S4.

Besides solvent mediation, it is expected that the different structural characteristics of self-assembled aggregate of *cis*- from *trans*- AOB-t8 could be distinguished in the molecular arrangement. From the electronic UV-vis absorption spectra of AOB-t8 in solution, the information about the aggregated state of azobenzene on molecular scale could be obtained. As shown in Fig. 5a, the absorption spectra of *trans*-AOB-t8 manifest a slight but detectable dependence on concentration in ETO. With the concentration increasing from $1\times10^{-5}$ M to $1\times10^{-3}$ M, the absorption maximum is slightly blue-shifted from 365 nm to 357 nm, indicating the formation of H-aggregates.[21,22] In other word, the observed quantum yield decreasing with concentration (Table S1) without UV irradiation could be attributed to concentration-quenching or the formation of H-aggregates. On the contrary, with UV light irradiation to balance state, the n-π* absorption maximum of *cis*- azobenzene group of AOB-t8 locates at 266 nm in a dilute ($1\times10^{-5}$ M) solution and red-shifts to 270 nm in the most concentrated solution ($1\times10^{-3}$ M). This spectroscopic difference for *cis*-AOB-t8 demonstrates that the azobenzene units are arranged into J-type aggregates through π-π interactions (Fig. 5b).[21,22] As a consequence, the fact that it contains mainly the H-aggregates might be the reason for a low quantum yield observed for the most concentrated solution ($1\times10^{-3}$ M) of *trans*-AOB-t8 in ETO. Accordingly, the high fluorescence quantum yield for the most concentrated solution ($1\times10^{-3}$ M) of *cis*-AOB-t8 could be attributed to the formation of J-aggregates, which could probably lead to the structural variety from fiber to plate related to different molecular conformation of AOB-t8.

**Table 2** Computed excitation energy (in eV) and oscillator strengths (in parenthesis) for the five lowest excited states of *trans*-AOB-t1 and *cis*-AOB-t1.

*trans*-AOB-t1

| Model | $S_1$ | | $S_2$ | $S_3$ | $S_4$ | $S_5$ |
|---|---|---|---|---|---|---|
| | GAS | ETO | | | | |
| B3LYP | 2.52 (0.00) | 2.58(0.00) | 2.87 (0.89) | 3.33 (0.03) | 3.36 (0.58) | 3.98 (0.14) |
| CAM-B3LYP | 2.79 (0.00) | 2.81(0.00) | 3.43 (1.59) | 4.29(0.25) | 4.51(0.05) | 4.57(0.01) |

*cis*-AOB-t1

| Model | $S_1$ | | $S_2$ | $S_3$ | $S_4$ | $S_5$ |
|---|---|---|---|---|---|---|
| | GAS | ETO | | | | |
| B3LYP | 2.45 (0.13) | 2.47(0.15) | 3.21 (0.21) | 3.59 (0.00) | 3.61 (0.34) | 3.92 (0.12) |
| CAM-B3LYP | 2.68 (0.06) | 2.74(0.09) | 4.09 (0.90) | 4.47 (0.20) | 4.60 (0.02) | 4.65 (0.02) |

**Theoretical study**

Theoretical calculations at DFT level were carried out to reveal the physical picture of the electronic excitation, excited state molecular geometry and the light emitting processes. To save the computational time, the 3,4,5-octanoxy group of AOB-t8 was replaced by a methoxy group (-$OCH_3$, AOB-t1, scheme 1). Table 2 listed the five lowest electronic transitions of AOB-t1 calculated with different functionals. The obtained results indicate that $S_0$ to $S_1$ transition of *trans*-AOB-t1 is not allowed (zero oscillator strengths), while $S_0$ to $S_2$ transition is highly allowed with non-zero oscillator strength of 1.59. The inclusion of solvent effects (ETO) by a PCM model gives a red-shift of these excitation energies. By comparing with experimental results, the best agreement can be found for CAM-B3LYP approaches. When a dilute ($1\times10^{-5}$ M) solution of *trans*-AOB-t8 in ETO is excited at 320 nm, $S_0$ to $S_2$ transition is highly allowed and $S_1$ state rarely populated. This is consistent with our experimental observation of a very weak fluorescence with a quantum yield of about $0.2\times10^{-2}$. These theoretical results also sustains that the two main bands of *trans*-AOB-t8 observed in UV-vis absorption spectra can be attributed to the transitions from ground state to $S_2$ and higher excited states, respectively. The lower energy band shows only π-π* character, while the higher energy band consists of several transitions, including both n-π* and π-π* type of transition. Fig. 6 and Fig. S5 presents the electronic density of frontier molecular orbitals of AOB-t1 involved in the five lowest transitions.

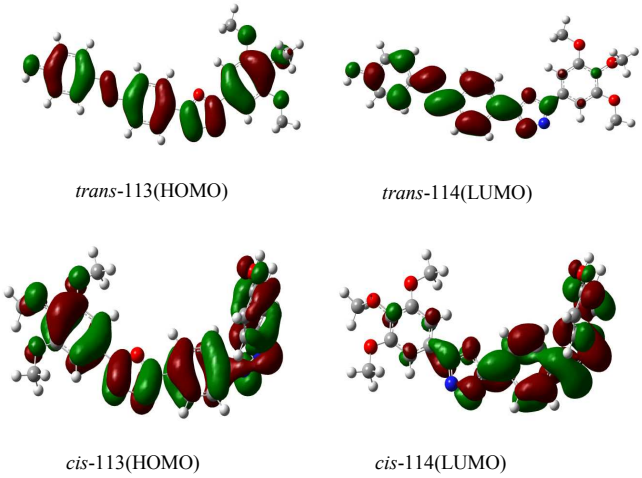


**Fig. 6** Electron density diagrams of molecular orbitals of *trans*-AOB-t1 and *cis*-AOB-t1 computed with CAM-B3LYP/6-31G** method.

According to the TD-CAM-B3LYP calculations, three lowest allowed transitions of *trans*-AOB-t1 are $S_2 \leftarrow S_0$ (3.43 eV, $f$=1.59), $S_3 \leftarrow S_0$ (4.29 eV, $f$=0.25) and $S_4 \leftarrow S_0$ (4.51 eV, $f$=0.05). An inspection of the component orbital transitions make it clear that the former two absorptions should be assigned as a π-π* type, where the first one is highly allowed and mainly consists of *trans*-113→*trans*-114 and *trans*-112→*trans*-114 transitions, while the second one is a combination of several transitions, mainly including *trans*-112→*trans*-114 and *trans*-109→*trans*-114, *trans*-113→*trans*-114. Orbital *trans*-113(HOMO) has the electron density localized on the azobenzene unit, and the electron density of orbital *trans*-114(LUMO) is delocalized slightly. Compared with the electronic transitions of *trans*-AOB-t1, $S_0$ to $S_1$ transition of *cis*-AOB-t1 is partially allowed with non-zero oscillator strengths of 0.15. When a dilute ($1\times10^{-5}$ M) solution of *cis*-AOB-t8 in ETO is excited at 320 nm, $S_0$ to $S_2$ transition is highly allowed and $S_1$ state is populated to a certain extent by internal conversion. Therefore, the absorption cross-section starts increasing with the UV light irradiation. According to the TD-CAM-B3LYP calculations, the three lowest allowed transitions of *cis*-AOB-t1 are $S_1 \leftarrow S_0$ (2.74 eV, $f$=0.09), $S_2 \leftarrow S_0$ (4.09 eV, $f$=0.9) and $S_3 \leftarrow S_0$ (4.47 eV, $f$=0.2). The component orbital transitions indicate that the former two emissions should be assigned as a π-π* type, where the first one is slightly allowed and mainly consist of *cis*-113→*cis*-114 and *cis*-109→*cis*-114 transitions, the second one is highly allowed and mainly including *cis*-113→*cis*-114, *cis*-113→*cis*-115 and *cis*-112→*cis*-115 transitions. Orbital *cis*-113(HOMO) has the electron density totally delocalized over the whole π-system, while orbital *cis*-114(LUMO) has the electron density localized on azobenzene and 1,3,4-oxadiazole units.

In the literature, Han and co-workers observed the photoinduced formation of blue fluorescent aggregates for simple azobenzene derivatives with different alkyl chain lengths, in which the isolated molecules in solution were nonfluorescent at ambient temperature. However, the work did not include the studies of physical origin and the detailed mechanism.[12] In contrast, a highly fluorescent self-assembled plate aggregate of AOB-t8 in organic solution under UV light illumination has been obtained, even though AOB-t8 itself is negligibly fluorescent in nonirradiated initial solution. Combining of spectroscopic techniques and theoretical calculations, we have discussed the mechanism for light-driven fluorescence and emission enhancement for the monomeric AOB-t8. The calculated results have been demonstrated a good consistence with the experimental observations. Summarily, in the diluted solution, the photoinduced emission enhancement arises from the isomerization of monomeric AOB-t8 from *trans*- to *cis*- conformation with the UV irradiation. This isomerization will then initializes the self-assembly aggregation of *cis*-AOB-t8 and intensifies further emission enhancement with increasing the irradiation time. In other word, the observed emission enhancement comprises both the contributions from monomeric and aggregated *cis*-AOB-t8. The results from morphology and spectroscopy studies on concentration dependence indicate the correlation between the emission properties and aggregate structures for AOB-t8 with and without UV irradiation. The H-aggregate molecular arrangement can interpret the nonfluorescence of *trans*-AOB-t8, and the formation of J-aggregation for *cis*-AOB-t8 could be the structural origination of aggregation-induced emission enhancement.

## Conclusion

The light-driven photophysical properties and structural characteristics activated by photoisomerization of AOB-t8 have been investigated systematically. Here, we represent the highly fluorescent self-assembled plate aggregates of an azobenzene molecule in organic solution under UV light illumination even though azobenzene itself is negligibly fluorescent in initial solution. The *trans*-to-*cis* photoisomerization of AOB-t8 by UV irradiation at 365 nm is followed by a florescent monomer and a significant emission enhancement due to the spontaneous formation of spherical aggregates. The results from theoretical calculation, spectroscopy and morphology studies are consistently used to clarify and clearly demonstrate the origination and mechanism for the emission enhancement of *cis*-AOB-t8 in mono-dispersed molecule and aggregated architecture, respectively. Without UV light irradiation, the quantum yield of the concentrated *trans*-AOB-t8 initially decreases with increasing concentration, and reaches $1.1\times10^{-3}$ due to the formation of H-aggregates. However, after UV light irradiation, the emission spectrum exhibits multiple emission bands and the quantum yield can be increased to $33.7\times10^{-2}$, corresponding to 306 times enhancement. The obtained results indicate that the photophysical properties of AOB-t8 are assuredly associated with the molecular conformation and aggregated structure. The structural evolution of fluorescent *cis*-AOB-t8 has been represented from monodispersed molecule to aggregated spherical nanoparticle, fiber-like aggregates and layer structure aggregates. With the combination of obtained

experimental data and theoretical results, we have discussed the mechanisms responsible for light-driven fluorescence, emission enhancement, and the aggregation-induced enhancement via J-aggregate arrangement for *cis*-AOB-t8, which have demonstrated a good consistency in this work.

## Materials and methods

### Experimental details

All the solvents for spectral measurements were of spectroscopic grade and used as received. Field emission scanning electron microscopy (FE-SEM) images were taken with a JSM-6700F apparatus. Samples for FE-SEM measurement were prepared by wiping a small amount of solution onto a silicon plate, and followed by drying in a vacuum for 12 h at room temperature. Photoirradiation was carried out with a 250 W super pressure Hg lamp through a lightguide and an appropriate color filter ($320 < \lambda < 390$ nm for UV light). The intensity of the UV was ca. 7500 mW $cm^{-2}$ at the tip of the lightguide. UV-vis absorption spectra were obtained on a Shimadzu UV-2550 spectrometer. Photoluminescence spectra were collected by a Perkin-Elmer LS55 spectrophotometer. The room-temperature luminescence quantum yields in solutions were determined relative to quinine sulfate in sulfuric acid aqueous solution (0.546), and calculated according to the equation: $\Phi_{unk}=\Phi_{std}(I_{unk}/A_{unk})(A_{std}/I_{std})(\eta_{unk}/\eta_{std})$[23], in which $\Phi_{unk}$ is the radiative quantum yield of the sample; $\Phi_{std}$ is the radiative quantum yield of the standard; $I_{unk}$ and $I_{std}$ are the integrated emission intensities of the sample and standard, respectively; $A_{unk}$ and $A_{std}$ are the absorptions of sample and standard at the excitation wavelength, respectively; $\eta_{unk}$ and $\eta_{std}$ are the indexes of refraction of the sample and standard solutions (pure solvents were assumed), respectively.[24] Fluorescence lifetimes were measured using FL920 time-correlated single photon counting (TCSPC) system.

### Theoretical calculation details

In theoretical calculation, the AOB-t8 was replaced by a methoxy group (AOB-t1, scheme 1) to save the computational time. The molecular structure of AOB-t1 in the ground state was optimized at DFT level based on two different groups of hybrid functionals, namely global hybrid (GH) and rang-separated hybrid (RSH) functionals. For the GH functionals, the percentage of Hartree-Fock exchange (HFE) was constant at each point in space. In the present work, GH has been selected as B3LYP (20% of HFE). For RSH functionals, the fraction of HFE increases with the inter-electronic distance, giving the so-called long range correction scheme. This group included CAM-B3LYP approach, where the HFE percentage smoothly increased from 19% to 65%.

The molecular geometries of AOB-t1 in the excited states were optimized by using the TD-CAM-B3LYP method. The excitation and emission energies were computed by TD-DFT approaches. In all calculations, standard 6-311+G** basis sets was applied. All these calculations were carried out with Gaussian 09 software package (version A.02).[25]

## Acknowledgements

The authors are grateful to the National Science Foundation Committee of China (project No. 21173068, 21373077) and the Program for Innovative Research Team in University of Henan Province (No. 13IRTSTHN017) for their financial support to this work.

## Notes and references

[a] Institute of Photobiophysics, School of Physics and Electronics, Henan University, Kaifeng 475004, People's Republic of China.
[b] Key Laboratory for Automobile Materials, Ministry of Education, Institute of Materials Science and Engineering, Jilin University, Changchun 130012, People's Republic of China.
† Corresponding author: juneguo@henu.edu.cn (L. G.).

Electronic Supplementary Information (ESI) available: [Fluorescence lifetime decay profiles (excitation at 295 nm) of AOB-t8 in different solvents. Photophysical characteristics of AOB-t8 ($1\times10^{-5}$ M and $1\times10^{-3}$ M) in ethanol at room temperature. The photophysical property and structural characteristics of AOB-t8 in dichloromethane. Electron density diagrams of molecular orbitals of *trans*-AOB-t1 and *cis*-AOB-t1 computed with CAM-B3LYP/6-31G** method.]. See DOI: 10.1039/b000000x/

1 (a) G. Kumar and D. C. Neckers, *Chem. Rev.*, 1989, **89**, 1915; (b) D. Brown, A. Natansohn and P. Rochon, *Macromolecules*, 1995, **28**, 6116; (c) S. J. Ziker, T. Bieringer, S. Haarer, R. S. Stein, J. W. van Egmond and S. G. Kostromine, *Adv. Mater.*, 1998, **10**, 855; (d) A. Natansohn and P. Rochon, *Chem. Rev.*, 2002, **102**, 4139; (e) J. A. Delaire and K. Nakatani, *Chem. Rev.*, 2000, **100**, 1817; (f) C. J. Barrett, J. Mamiya, K. G. Yagerc and T. Ikeda, *Soft Matter*, 2007, **3**, 1249; (g) Y. Zhao and J. He, *Soft Matter*, 2009, **5**, 2686.

2 (a) W. M. Gibbons, P. J. Shannon, S. T. Sun and B. J. Swetlin, *Nature*, 1991, **351**, 49; (b) S. Peng, Q. Guo, P. G. Hartley and T. C. Hughes, *J. Mater. Chem. C*, 2014, **2**, 8303; (c) D. Hore, A. Natansohn and P. Rochon, *J. Phys. Chem. B*, 2003, **107**, 2197; (d) H. R. Hafiz and F. Nakanishi, *Nanotechnology*, 2003, **14**, 649; (e) P. H. Rasmussen, P. S. Ramanujam, S. Hvilsted and R. H. Berg, *J. Am. Chem. Soc.*, 1999, **121**, 4738.

3 (a) E. Ishow, B. Lebon, Y. N. He, X. G. Wang, L. Bouteiller, L. Galmiche and K. Nakatani, *Chem. Mater.*, 2006, **18**, 1261; (b) B. L. Lachut, S. A. Maier, H. A. Atwater, M. J. A. de Dood, A. Polman, R. Hagen and S. Kostromine, *Adv. Mater.*, 2004, **16**, 1746; (c) Q. Zeng, Z. A. Li, Z. Li, C. Ye, J. G. Qin and B. Z. Tang, *Macromolecules*, 2007, **40**, 5634; (d) L. He, G. Wang, Q. Tang, X. Fu and C. Gong, *J. Mater. Chem. C*, 2014, **2**, 8162.

4 (a) X. B. Chen, Y. H. Zhang, B. J. Liu, J. J. Zhang, H. Wang, W. Y. Zhang, Q. D. Chen, S. H. Pei and Z. H. Jiang, *J. Mater. Chem.*, 2008, **18**, 5019; (b) S. Chen, C. Chu and V. K. S. Hsiao, *J. Mater. Chem. C*, 2013,**1**, 3529; (c) D. R. Wang, G. Ye, Y. Zhu and X. G. Wang, *Macromolecules*, 2009, **42**, 2651; (d) Q. Kulikovska, L. M. Goldenberg, L. Kulikovsky and

J. Stumpe, *Chem. Mater.*, 2008, **20**, 3528; (e) Z. Li, W. Wu, C. Ye, J. Qin and Z. Li, *Polym. Chem.*, 2010, **1**, 78.
5 A. Cembran, F. Bernardi, M. Garavelli, L. Gagliardi and G. Orlandi, *J. Am. Chem. Soc.*, 2004, **126**, 3234.
6 H. Rau, *Angew. Chem., Int. Ed. Engl.*, 1973, **12**, 224.
7 C. H. Tung and J. Q. Guan, *J. Org. Chem.*, 1996, **61**, 9417.
8 Z. Lei, A. Vaidyalingam and P. K. Dutta, *J. Phys. Chem. B*, 1998, **102**, 8557.
9 (a) J. Yoshino, A. Furuta, T. Kambe, H. Itoi, N. Kano, T. Kawashima, Y. Ito, and M. Asashima, *Chem. Eur. J.*, 2010, **16**, 5026. (b) J. Yoshino, N. Kano, T. Kawashima, *Dalton Trans.*, 2013, **42**, 15826.
10 M. Shimomura and T. Kunitake, *J. Am. Chem. Soc.*, 1987, **109**, 5175.
11 K. Tsuda, G. C. Dol, T. Gensch, J. Hofkens, L. Latterini, J. W. Weener, E. W. Meijer and F. C. Schryver, *J. Am. Chem. Soc.*, 2000, **122**, 3445.
12 M. Han and M. Hara, *J. Am. Chem. Soc.*, 2005, **127**, 10951.
13 M. Han, Y. Hirayama and M. Hara, *Chem. Mater.*, 2006, **18**, 2784.
14 P. S. Zacharias, S. Ameerunisha, S. R. Korupoju, *J. Chem. Soc. Perkin Trans.,* 1998, **2**, 2055.
15 P. Smitha, S. K. Asha, *J. Phys. Chem. B* 2007, **111**, 6364.
16 Q. Bo, Y. Zhao, *Langmuir,* 2007, **23**, 5746.
17 (a) J. Xu, W. Zhang, N. C. Zhou, J. Zhu, Z. P. Cheng, Y. Xu, X. L. Zhu, *J. Polym. Sci. A: Polym. Chem.,* 2008, **46**, 5652; (b) Y. Xiang, X. Q. Xue, J. Zhu, Z. B. Zhang, W. Zhang, N. C. Zhou, X. L. Zhu, *Polym. Chem.,* 2010, **1**, 1453.
18 X. Ran, H. Wang, J. Lou, L. Shi, B. Liu, M. Li, and L. Guo, *Soft Materials*, 2014, **12**, 396.
19 R. Métivier, R. Amengual, I. Leray, V. Michelet, J. -P. Genêt, *Org. Lett.* 2004, **6**, 739.
20 M. Han and K. Ichimura, *Macromolecules*, 2001, **34**, 82.
21 M. Shimomura and T. Kunitake, *J. Am. Chem. Soc.*, 1987, **109**, 5175.
22 H. Kobayashi, K. Koumoto, J. H. Jung and S. Shinkai, *J. Chem. Soc., Perkin Trans.,* 2002, **2**, 1930.
23 (a) C. W. Tang and S. A. VanSlyke, *Appl. Phys. Lett.*, 1987, **51**, 913; (b) J. H. Burroughes, D. D. C. Bradley, A. R. Brown, R. N. Marks, R. H. Friend, P. L. Burn and A. B. Holmes, *Nature*, 1990, **347**, 539.
24 K. Q. Ye, J. Wang, H. Sun, Y. Liu, Z. C. Mu, F. Li, S. M. Jiang, J. Y. Zhang, H. X. Zhang, Y. Wang and C. M. Che, *J. Phys. Chem. B*, 2005, **109**, 8008.
25 M. J. Frisch, G. W. Trucks, H. B. Schlegel, G. E. Scuseria, M. A. Robb, J. R. Cheeseman, G. Scalmani, V. Barone, B. Mennucci, G. A. Petersson, H. Nakatsuji, M. Caricato, X. Li, H. P. Hratchian, A. F. Izmaylov, J. Bloino, G. Zheng, J. L. Sonnenberg, M. Hada, M. Ehara, K. Toyota, R. Fukuda, J. Hasegawa, M. Ishida, T. Nakajima, Y. Honda, O. Kitao, H. Nakai, T. Vreven, J. A. Montgomery, J. E. Peralta, F. Ogliaro, M. Bearpark, J. J. Heyd, E. Brothers, K. N. Kudin, V. N. Staroverov, R. Kobayashi, J. Normand, K. Raghavachari, A. Rendell, J. C. Burant, S. S. Iyengar, J. Tomasi, M. Cossi, N. Rega, J. M. Millam, M. Klene, J. E. Knox, J. B. Cross, V. Bakken, C. Adamo, J. Jaramillo, R. Gomperts, R. E. Stratmann, O. Yazyev, A. J. Austin, R. Cammi, C. Pomelli, J. W. Ochterski, R. L. Martin, K. Morokuma, V. G. Zakrzewski, G. A. Voth, P. Salvador, J. J. Dannenberg, S. Dapprich, A. D. Daniels, Ö. Farkas, J. B. Foresman, J. V. Ortiz, J. Cioslowski and D. J. Fox, GAUSSIAN 09 (Revision A.02), Gaussian, Inc., Wallingford, CT, 2009.

# Table of Contents Graphic

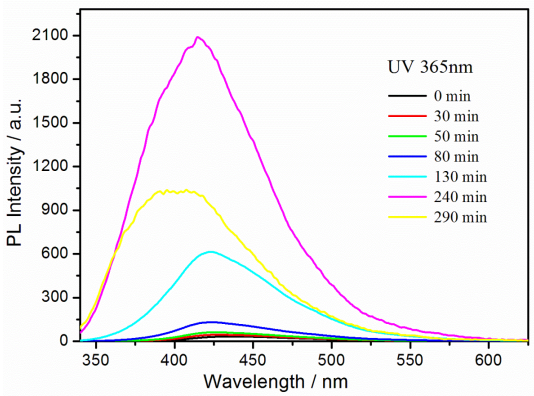


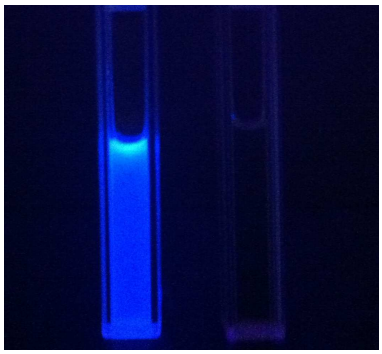

Light-driven fluorescence and emission enhancement of AOB-t8 in organic solution under UV light illumination was obtained, even though AOB-t8 itself is negligibly fluorescent in nonirradiated initial solution.